Journal of Geophysical Research: Solid Earth

Supporting Information for

Along-Strike Variations of Alaska Subduction Zone Structure and Hydration Determined From Amphibious Seismic Data

Zongshan Li[1], Douglas A. Wiens[1], Weisen Shen[2], Donna J. Shillington[3]

[1]Department of Earth, Environmental, and Planetary Sciences, Washington University, St. Louis, MO 63130, USA.

[2]Department of Geosciences, Stony Brook University, Stony Brook, NY 11794, USA.

[3]School of Earth and Sustainability, Northern Arizona University, Flagstaff, AZ 86011, USA.

Corresponding author: Zongshan Li (zongshan.li@wustl.edu)

Contents of this file

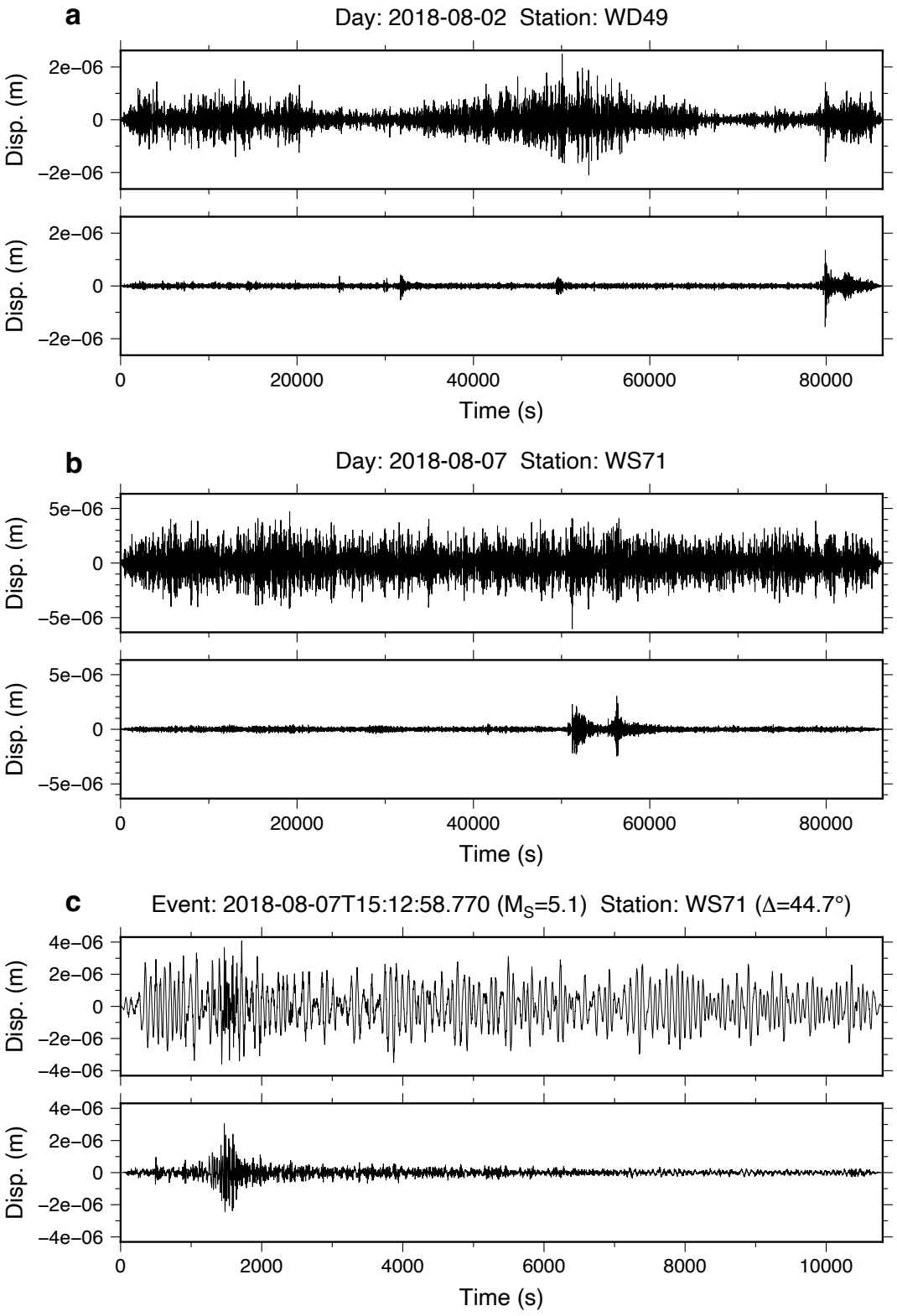

Figure S1. Examples of tilt and compliance noise removal for ocean bottom seismograph (OBS) vertical component records in displacement units. All waveforms are plotted after

applying a bandpass filter between 10 and 100 s. **(a)** Daily length seismic waveform of AACSE OBS WD50 on 2018-08-02, which is dominated by tilt noises on the raw waveform (upper) but has few noises after correction (lower). **(b)** Daily length seismic waveform of AACSE OBS WS71 on 2018-08-07, an example that has strong compliance noises on the raw waveform (upper) and denoised after correction (lower). **(c)** A 10800 s length seismic waveform of the 2018-08-07T15:12:58.770 M_S = 5.1 event recorded by AACSE OBS WS71, which is a segment cut from (b). The distinct contrast before (upper) and after (lower) the noise removal suggests that noise correction is very helpful in improving surface wave signals that are obscured by the ocean bottom noises, which is especially important for smaller earthquakes recorded by OBS.

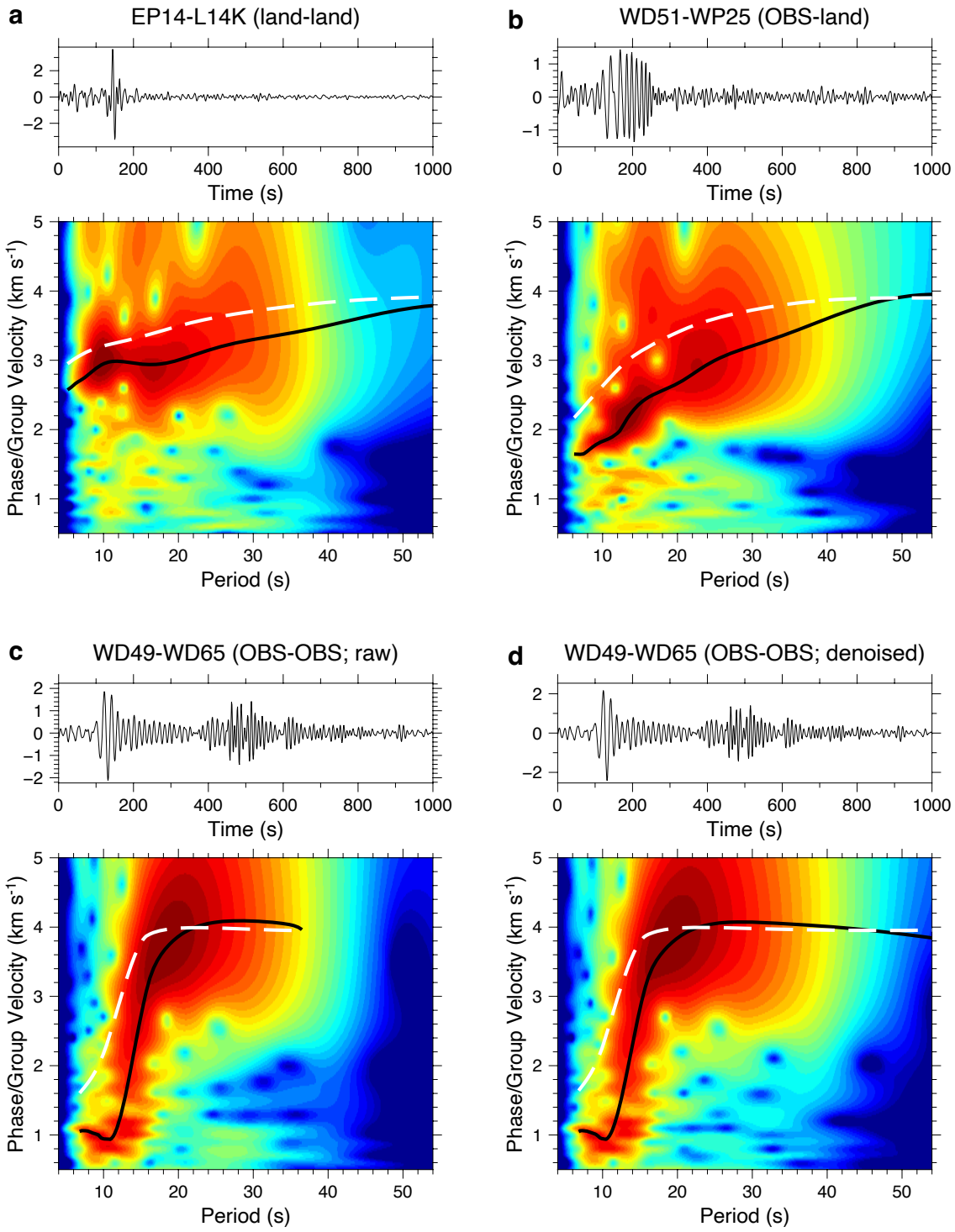

Figure S2. Examples of ambient noise cross-correlations and frequency-time analysis (FTAN) measurements for land-land pairs, OBS-land pairs, and OBS-OBS pairs, respectively. All waveforms (upper) are plotted after a bandpass filter between 8 and 36 s. All spectrums (lower) are plotted following the narrow bandpass Gaussian filtering of FTAN, with the measured group velocity dispersion curves shown as solid black lines and

corresponding phase velocity dispersion curves shown as dashed white lines. **(a)** A land-land station pair between land stations EP14 and L14K, which has typical continental waveforms and dispersion curves. **(b)** An OBS-land station pair between OBS WD51 and land station WP25, which has lower velocities at shorter periods compared with the land-land pairs. **(c)** An OBS-OBS pair using raw waveforms between OBSs WD49 and WD65, which has typical oceanic dispersion curves. **(d)** An OBS-OBS pair using denoised waveforms between denoised waveforms OBS WD49 and WD65. It also shows typical oceanic dispersion curves, but with stronger signals at longer periods and achieves measurements at periods > 40 s.

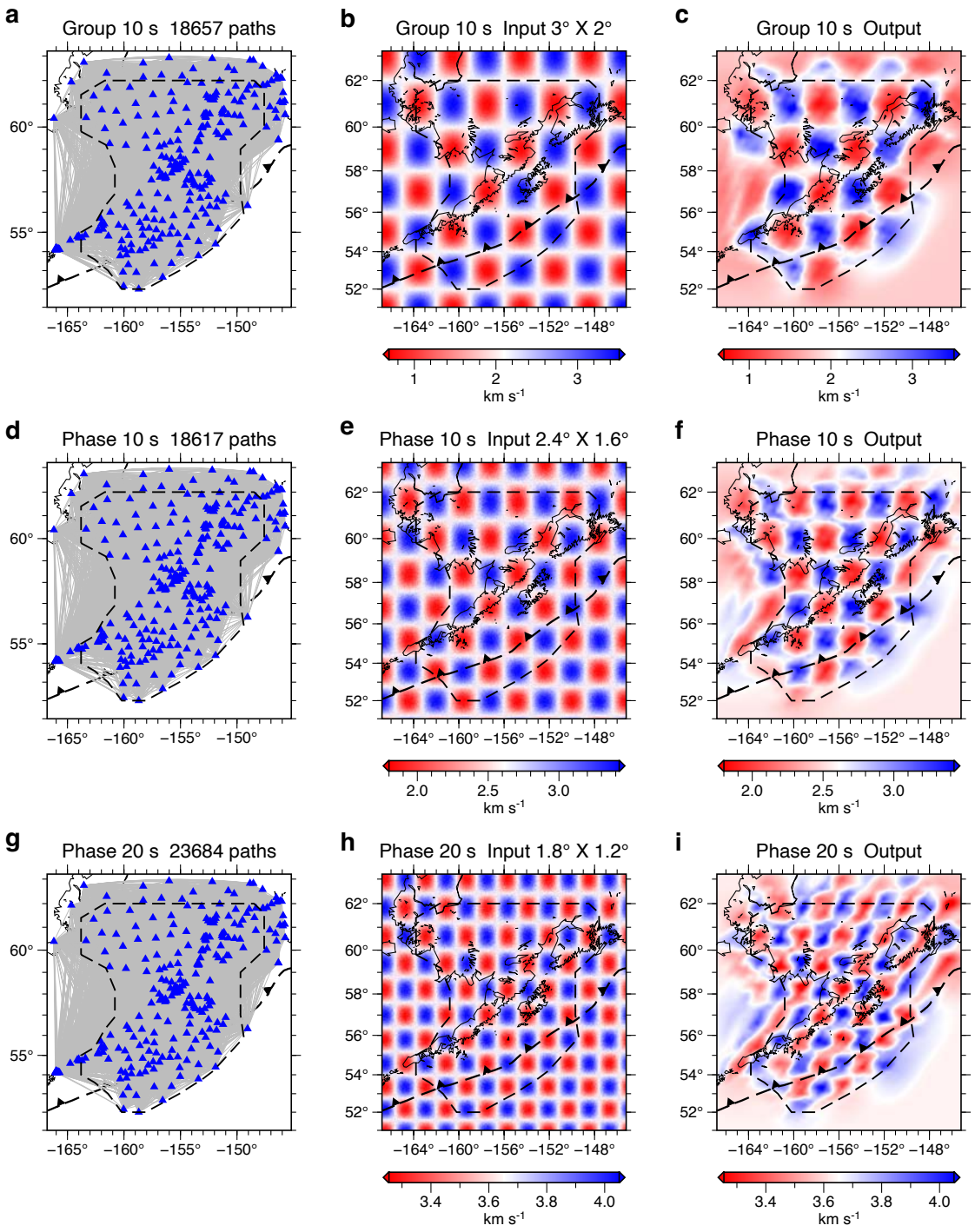

Figure S3. Checkerboard resolution tests of ambient noise tomography (ANT). Examples are shown for group and phase velocity at 10 s, and phase velocity at 20 s. The results suggest that resolution depends on the velocity range, noise perturbation, and ray path coverage. The parameters of 0.3°×0.2° grid spacing and 0.5° isotropic cells are reasonable to apply ambient noise tomography. **(a-c)** The group velocity at 10 s has 18657 paths and could recover 3°×2° checkerboards after ANT. To make the input model

close to real data, we add some Gaussian noises with std = 0.10 km s^{-1} to the checker velocities. **(d-f)** The phase velocity at 10 s has 18617 paths and could recover 2.4°×1.6° checkerboard, with some Gaussian noises of std = 0.10 km s^{-1} added. **(g-l)** The phase velocity at 20 s has 23684 paths and could recover 1.8°×1.2° checkerboard, with some Gaussian noises of std = 0.05 km s^{-1} added.

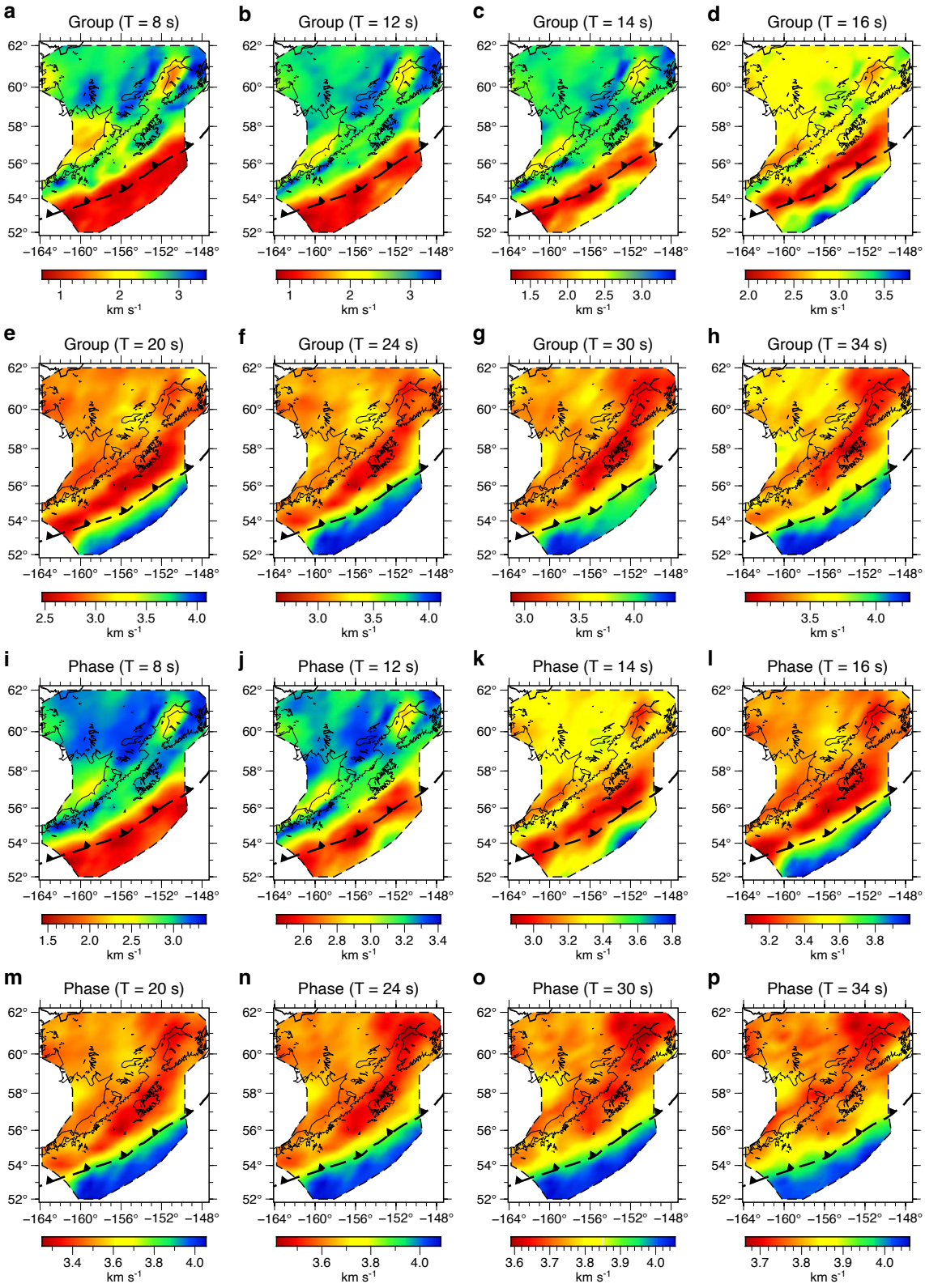

Figure S4. Rayleigh wave group and phase velocity maps from ambient noise tomography (ANT). The dashed black contour indicates our study area with reliable

results. At short periods (8-14 s), the group and phase velocity maps reflect the very shallow structure and water depth, where incoming plate and trench are dominated by low-speed anomalies and mountain ranges show high-speed anomalies. At longer periods (20-30 s), the group and phase velocity maps reflect the crust and uppermost mantle structure, where the incoming plate is dominated by high-speed anomalies and low-speed anomalies cover the forearc region. **(a-h)** Group velocity maps from 8 to 34 s. **(i-p)** Phase velocity maps from 8 to 34 s.

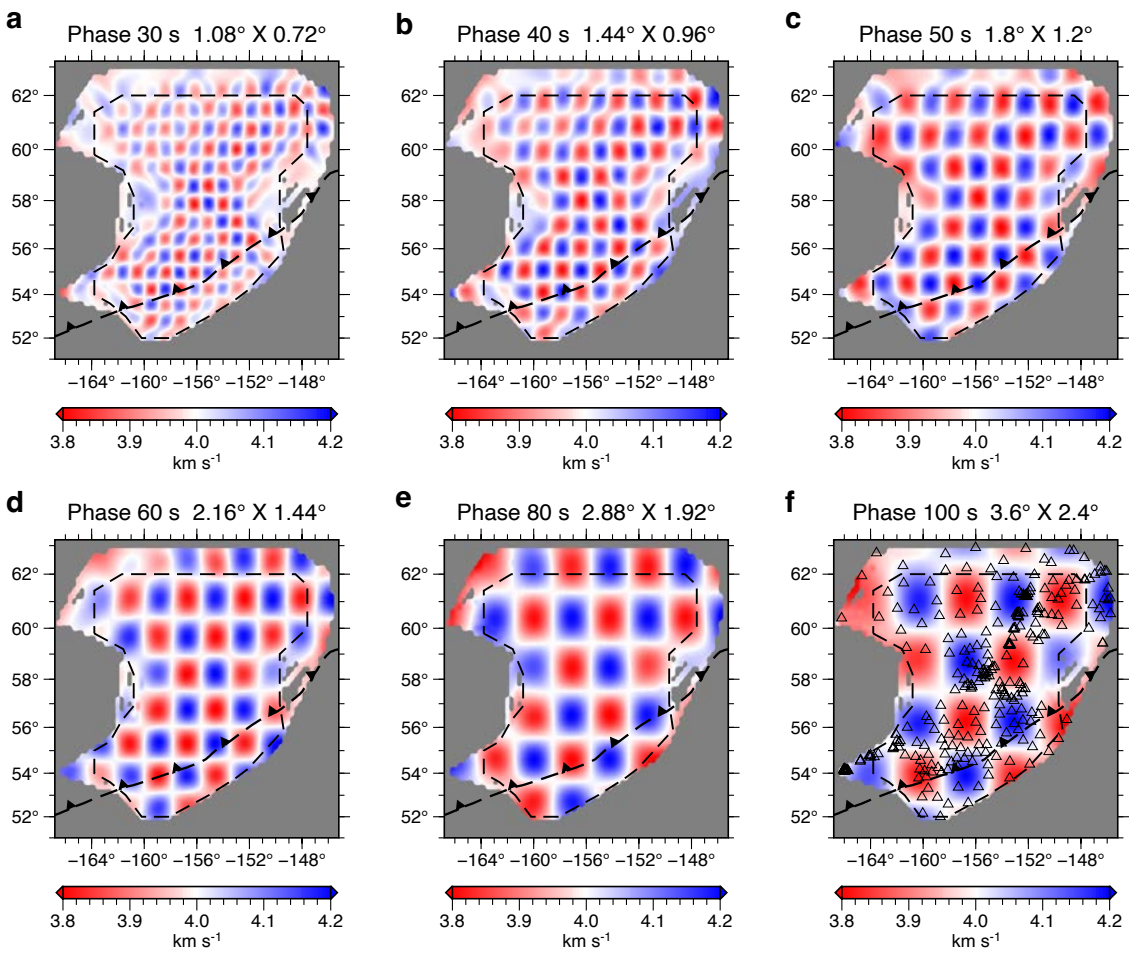

Figure S5. Checkerboard resolution tests of teleseismic Eikonal tomography (ET), which are for Rayleigh phase velocity at some example periods. The dashed black contour indicates our study area chosen to invert for 3-D V_{SV} model. **(a-f)** Phase velocity checkerboard tests at 30, 40, 50, 60, 80, 100 s, respectively. The checker size is approximately the Rayleigh wavelength, ranging from 1.08°×0.72° at 30 s to 3.6°×2.4° at 100 s. To make the input model close to real data, we add some Gaussian noises with std = 0.025 km s^{-1} to the checker velocities. The distribution of stations is marked in **(f)**. The grid spacing is 0.3°×0.2° and multichannel cross-correlations is performed for station pairs within 410 km. The results suggest that above parameters work well to recover the input anomalies.

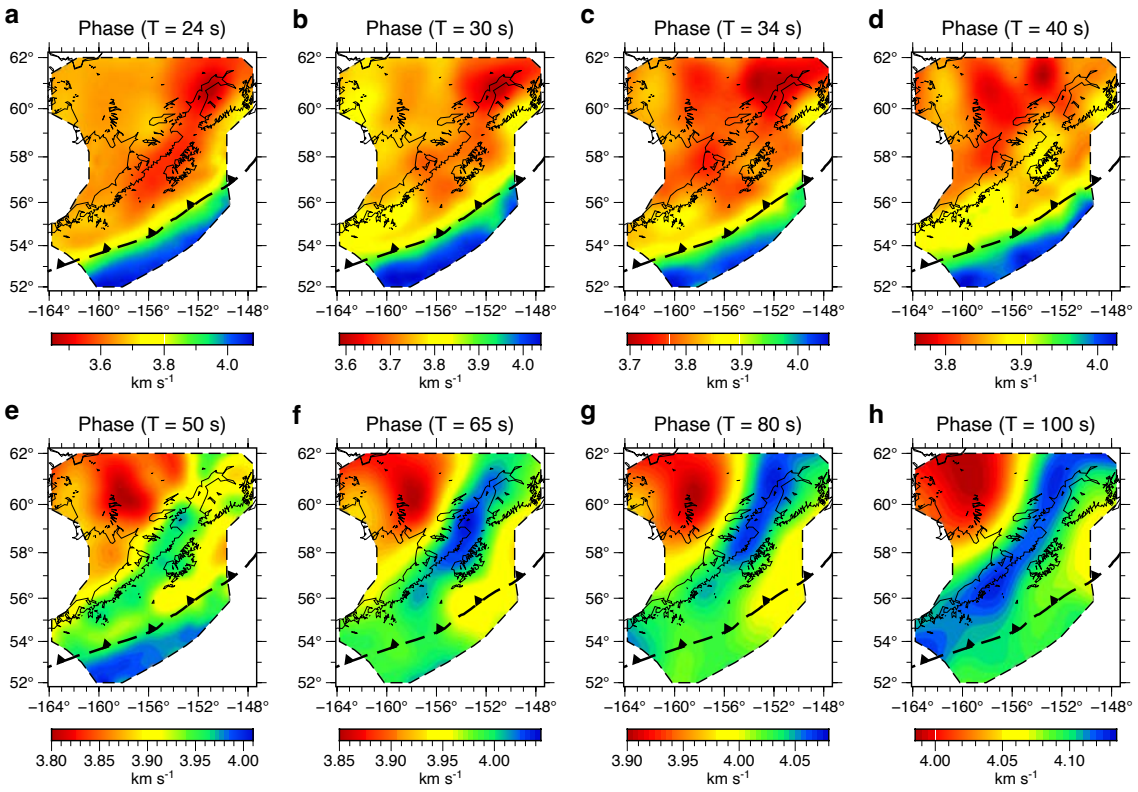

Figure S6. Rayleigh wave phase velocity maps from teleseismic Helmholtz tomography (HT) at example periods. The dashed black contour is determined by the region with reliable results. **(a-h)** Rayleigh wave phase velocity maps at 24 s to 100 s from HT. These phase velocity maps constrain the lower crust and uppermost mantle structure. At 40 s period, the high-velocity anomalies still dominate the incoming plate region and also extend north across the Aleutian Trench a little bit compared to the 24 s phase velocity map. At even longer periods (e.g., 60, 100 s), the trench region is replaced by low velocity, and high-speed anomalies gradually occupy the volcanic arc.

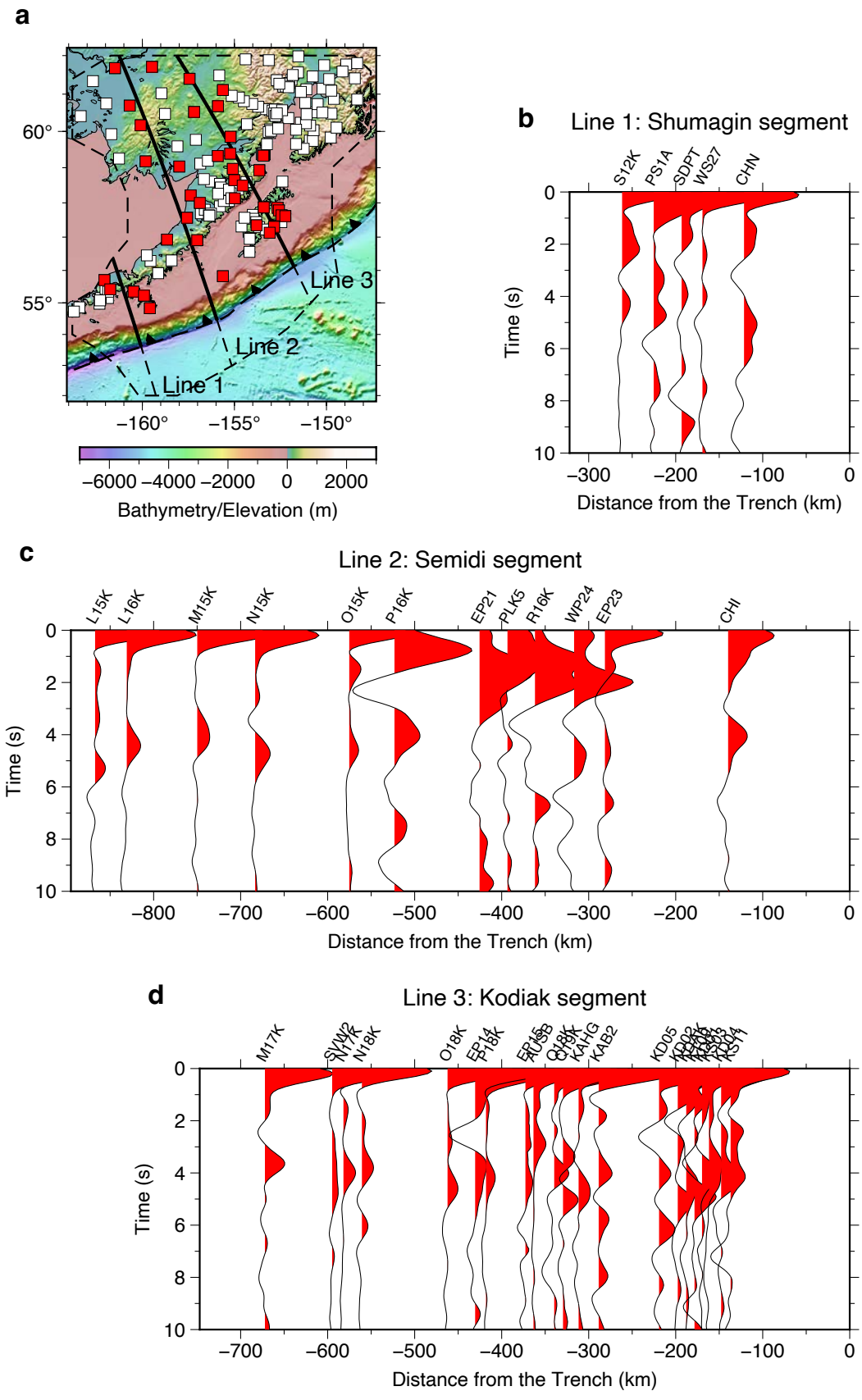
a
60°
55°
Line 3
Line 2
Line 1
−160°
−155°
−150°
−6000 −4000 −2000 0 2000
Bathymetry/Elevation (m)
b
Line 1: Shumagin segment
S12K
PS1A
SDPT
WS27
CHN
Time (s)
Distance from the Trench (km)
c
Line 2: Semidi segment
L15K
L16K
M15K
N15K
O15K
P16K
EP21
PLK5
R16K
WP24
EP23
CHI
Time (s)
Distance from the Trench (km)
d
Line 3: Kodiak segment
M17K
N18K
O18K
KAHG
KAB2
KD05
Time (s)
Distance from the Trench (km)

Figure S7. P-wave receiver functions (PRFs) of stations along profiles. **(a)** Location of three lines on the bathymetry and elevation map. The Line 1, 2, and 3 here are the same as that in **Figure 7**. Since there is no PRF for the incoming plate region, only the solid line segments are shown in the following profiles. All the 180 stations that contribute to the joint inversion are marked as rectangles, where those used in the following profiles are in red and others are in white. **(b-d)** The station PRFs along each profile. The x-axis is the distance relative to the trench axis with a positive distance in the direction of the incoming Pacific plate. The records of nearby PRFs for each line are shown along the distance from the Trench, with the station code labeled on the top. Here we define nearby PRFs as those within a distance of 75 km from the projection line. To avoid overlapping of clustered PRFs, we only keep the nearest one if there are multiple nearby PRFs within a 10 km interval of the distance from the Trench. The stacked PRFs of stations along the profile suggest that the overall quality of the PRFs is reasonably good to constrain the incoming plate Moho and/or the overriding plate Moho.

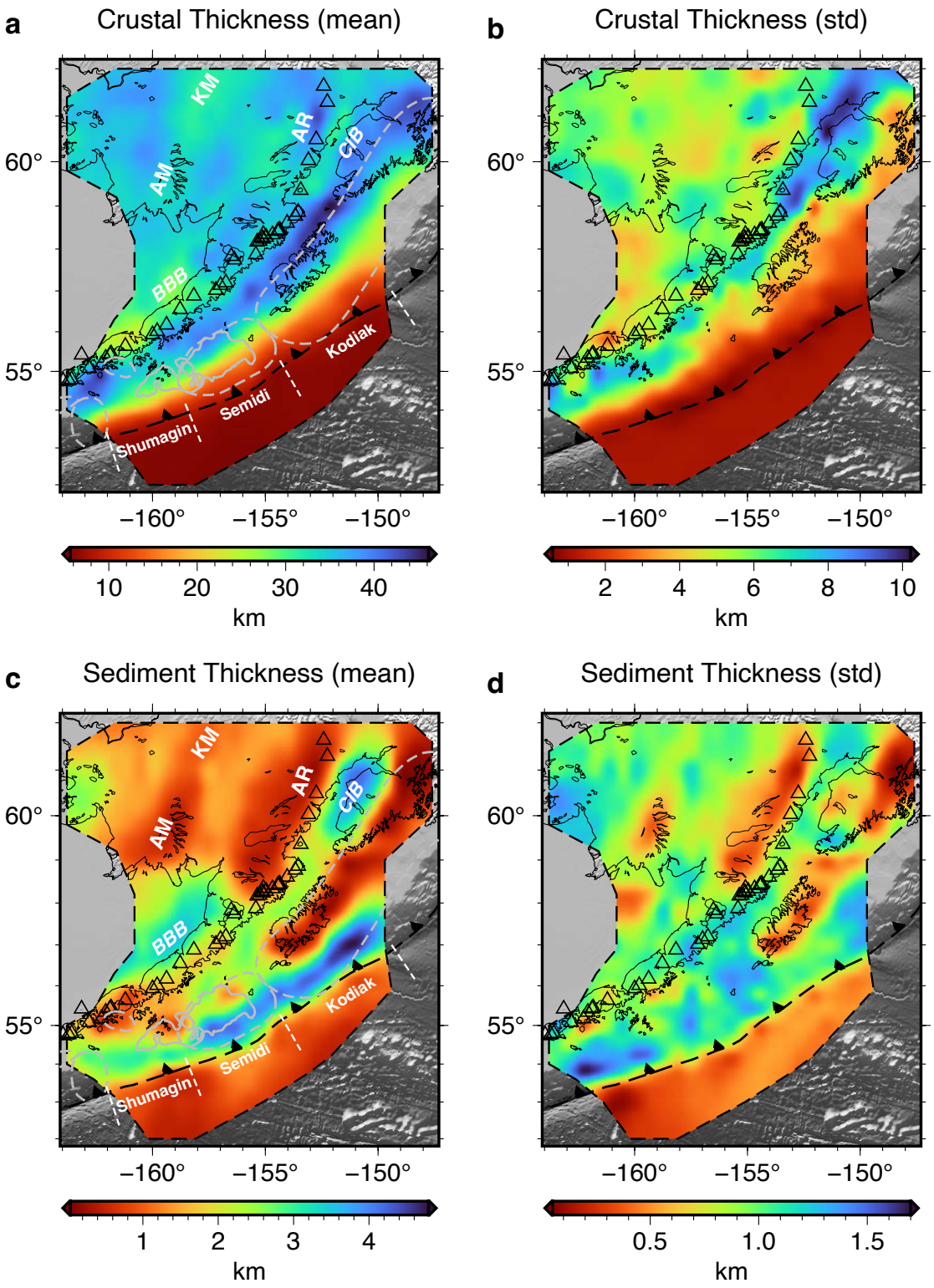

Figure S8. Map views of the posterior distribution for the crustal thickness and sediment thickness from surface wave inversion only. The comparison between the uncertainty map from surface wave inversion only and the final uncertainty map with joint inversion

results included (**Figure 5**) clearly shows how the PRFs help reduce uncertainty. The background image is the topography/bathymetry in gray scales. **(a)** Map view of the mean of the crustal thickness. The dashed gray lines are the contours of earthquake rupture zones shown in Figure 1b. The dashed white lines marked the range of Shumagin, Semidi, and Kodiak segments. Annotation of geological features: AM = Ahklun Mountains; KM = Kuskokwim Mountains; AR = Alaska Range; BBB = Bristol Bay Basin; CIB = Cook Inlet Basin. **(b)** Map view of the uncertainty of the crustal thickness. **(c)** Map view of the mean of the sediment thickness. Other labels are the same as that in (a). **(d)** Map view of the uncertainty of the sediment thickness.